THE STRUCTURE OF ONTOGENETIC VARIATION IN THE SHELL OF *PECTEN*

by SPAFFORD C. ACKERLY

ABSTRACT. Shell growth in *Pecten* conforms closely to a model where the shell margin is a sector of an ellipse (nearly circular), and where shell growth reflects an expansion and migration of the margin away from the shell apex. Detailed ontogenetic measurements on seven species ($n = 23$) indicate that all specimens are allometric, as reflected in both (1) a curvature of the ribs on the flattened left valve, and (2) a doming or vaulting of the coiled right valve. Patterns of covariation between growth parameters indicate that shell morphologies converge towards specific adult geometries. For example, juvenile shells with small length to height (L/H) ratios tend to become more elongate during growth (L/H increases) whereas juveniles with large L/H ratios tend to become shortened during growth (L/H decreases). These covariation patterns may represent morphogenetic processes which constrain adult morphologies to specific functional geometries.

GENERALIZATIONS are fundamental to an understanding of biological diversity, an excellent example being the log-spiral model of shell growth which has greatly enhanced our understanding of geometric diversity in molluscs. Most coiled shells fit, more or less, the log-spiral model (e.g. Raup 1966). However generalizations also obscure the underlying richness of actual data. Molluscs, for example, often do not grow in conformity with the spiral model (e.g. Schindel 1990). It is often the deviations from the ideal model which yield insights into the underlying biological aspects of shell growth and form.

The bivalve *Pecten* is ideally suited for a careful, empirical analysis of molluscan growth patterns. Not only is one valve approximately flat, and thus geometrically simple, but also growth in *Pecten* is generally allometric, as reflected in the curved ribs on the flattened, left valve (Text-fig. 1A). Measurements of rib positions and growth lines on the flattened valve, and of the spiral geometry on the convex right valve, give a detailed image of the patterns of growth observed within the genus. A growth model developed from the empirical measurements allows characterization of the varieties of allometry present in *Pecten*. Analysis of ontogenetic data suggests that the range of variation in *Pecten* (both inter- and intraspecific) is constrained to certain combinations of parameters, and that these combinations reflect morphogenetic and/or functional constraints on shell growth.

In subsequent sections, I will (1) summarize a procedure for analysing growth patterns in *Pecten*, (2) discuss the analysis of ontogenetic variation and allometry, (3) give details of a measurement protocol for *Pecten*, and (4) present an analysis of shell growth in 23 *Pecten* specimens.

ANALYSING GROWTH

Growth models for molluscs generally distinguish between the shape of the shell aperture (the 'generating curve') and the aperture's path (e.g. Raup 1966; Ackerly 1989). In *Pecten* species, the shape of the shell aperture, or shell margin, conforms closely to a sector of an ellipse (Text-figs 1–2), and a method for finding the lengths of the ellipse axes, and the location of the ellipse centre, is specified below (see Methods). On the flattened left valve of *Pecten*, growth occurs as the elliptical margin migrates away from the shell apex, the migration occurring in the plane of the page (Text-fig. 1). Growth in the convex right valve follows a similar migratory pattern, but in this case the aperture is also rotating to produce a spiral.

The empirical analysis of growth requires spatial (x,y,z) data on the positions of points on the

[Palaeontology, Vol. 35, Part 4, 1992, pp. 847–867.]

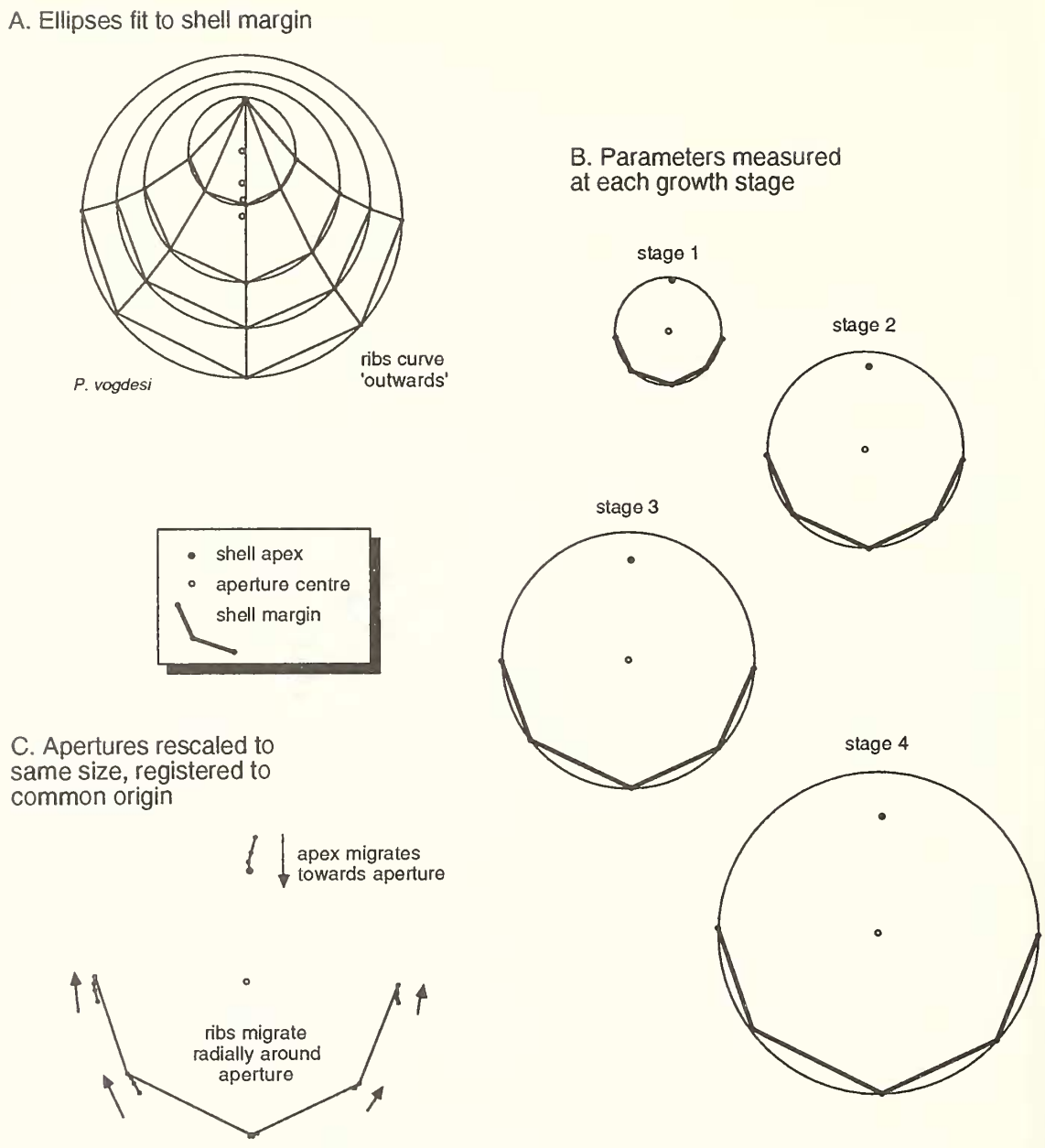

TEXT-FIG. 1. Growth patterns in *Pecten* (illustrated in *P. vogdesi*). A, ellipses are fitted to successive apertures. The small circles mark the best-fit ellipse centres. Ribs curve 'outwards' in the specimen. B, each growth stage is illustrated separately, with the best-fit ellipse to the shell margin, and a filled circle marking the position of the shell apex. C, the growth stages are rescaled to the same size (*r* is the size measure) and registered to a common origin defined by the aperture centre. The outline of the last growth stage is indicated, with dots marking the position of ribs. Line segments connect successive rib positions. A line segment connects apex positions (the heavy dot is the apex position of the final growth stage). If growth stages are isometric, then successive rib and apex positions will coincide. Allometries are indicated by (1) relative changes in the position of the apex, and (2) relative changes in rib position. In this specimen, the apex migrates towards the aperture, and ribs migrate radially around the margin.

shell margin at successive growth stages. The flattened left valve of *Pecten* is ideal because ribs and growth lines provide well-defined landmarks on a roughly two-dimensional surface. In the empirical analysis, ellipses are fitted to successive shell margins, and the centre of each ellipse marks the centre of the aperture (Text-fig. 1). The aspect ratio (a/b) defines the shape of each ellipse, and the radius (r) defines its size (the equation for an ellipse is: $x^2/a^2+y^2/b^2 = r^2$) (Text-fig. 2). The aspect ratio in an isometric shell will remain constant with size.

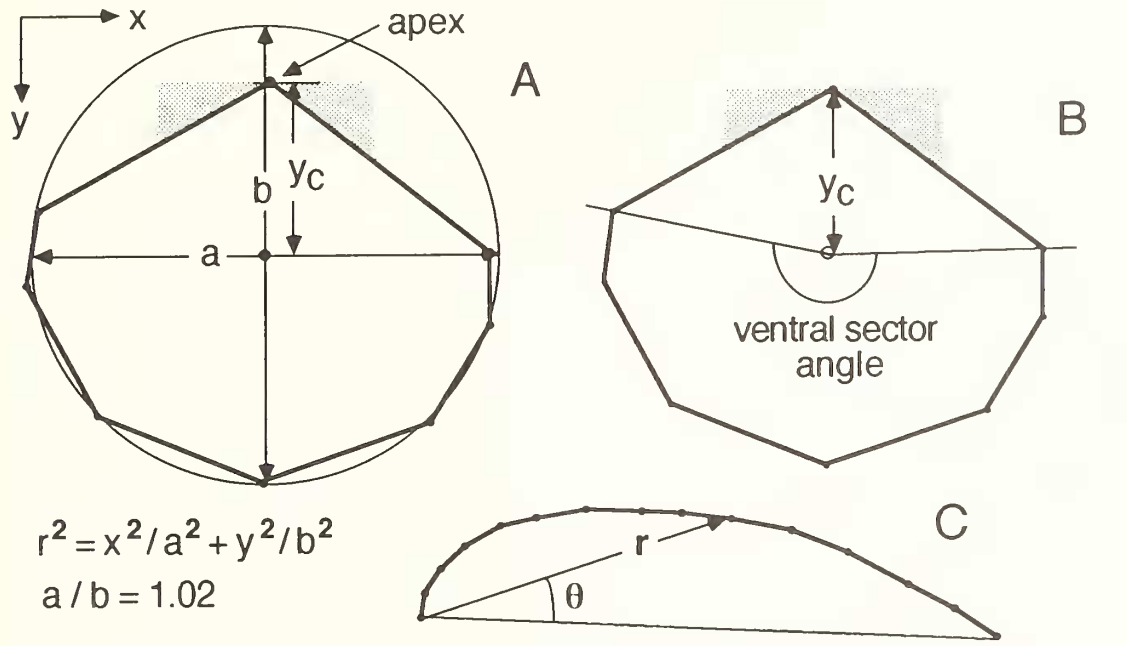

TEXT-FIG. 2. Parameters calculated by the computer algorithm for each growth stage. A, the position and aspect ratio of the ellipse which best fits the ventral shell margin. The ellipse radius defines the size, where: $r^2 = x^2/a^2+y^2/b^2$. The shell is oriented with the hinge line approximately parallel to the x-axis. y_c is the position of the ellipse centre measured in the y direction. B, the ventral sector is the angle subtending the ventral shell margin. C, the spiral geometry is measured in radial coordinates from an origin at the shell apex.

During growth, the aperture expands and migrates away from the shell apex (Text-fig. 1A–B). The relative position of the aperture and apex is readily visualized by rescaling successive apertures to the same size (r is the size measure) and registering them to a common origin (the aperture centre) (Text-fig. 1C). The rescaled figures for a *P. vogdesi* specimen (Text-fig. 1C) show that the aperture has, in a relative sense, migrated towards the apex during growth. The rescaled apertures in Text-figure 1C also show that the ribs are displaced radially around the shell margin during growth, migrating in the dorsal direction. The radial displacement is recorded by an increase in the ventral sector angle (see Text-fig. 2B) during growth.

A final component of *Pecten* morphology is related to the spiral geometry of the convex right valve. The spiralled shell morphology is very similar to the morphology of the flattened valve, but with a rotation of the aperture around a coiling axis, which in this case coincides with the shell apex. The rotation is expressed by the angular position (θ) and radius (r) of successive points on the spiral (Text-fig. 2C). The rate of increase of the radius defines the shell's radial expansion rate (σ) or, after Raup (1966), the whorl expansion rate (W), where W is the relative expansion after a complete 360° whorl ($W = e^{2\pi\sigma}$). When σ or W are large, the shell expands rapidly and is loosely coiled, whereas when σ or W are small, the shell expands slowly and is tightly coiled.

In summary, four parameters are sufficient to describe most of the shape variation in *Pecten* (Text-fig. 2): (1) the aspect ratio defines the shape of the elliptical margin; (2) the relative distance of the ellipse centre from the apex defines the aperture position; (3) the ventral sector angle specifies the arc length of the shell margin along the ellipse; and (4) the radial, or whorl, expansion rate defines the spiral geometry of the convex right valve. These parameters are measured at successive growth stages to estimate ontogenetic variations in *Pecten* shell morphology.

ONTOGENETIC VARIATION AND ALLOMETRY

Allometric growth, in which shape varies with size, is common in *Pecten*, and is represented by variations in the values of the growth parameters. Ontogenetic variations are illustrated for the specimen of *P. vogdesi* in Text-figure 1. The aspect ratio of the elliptical margin generated for *P. vogdesi* decreases from 1·007 in the first growth stage to 0·997–0·998 in subsequent growth stages (Text-fig. 3A). The overall trend in the aspect ratio is represented by a regression trend (Text-fig. 3A), although the significance of the trend is low because of the small number of points. Nevertheless, ontogenetic variations in the aspect ratio are common (see below). Note that the shape of the shell margin is very nearly circular ($a/b \approx 1$).

The relative position of the apex and shell aperture is expressed by a logarithmic relationship between aperture position and aperture radius (Text-fig. 3B). A slope of one (determined by reduced major axis regression) for this function indicates an isometric relationship. In the *P. vogdesi* specimen, however, the slope of 0·76 indicates that the apex–aperture distance increases less rapidly than aperture size, and the aperture centre migrates relatively towards the apex during growth (Text-fig. 1B–C).

The ventral sector angle increases consistently during growth, from a value of about 2·87 radians (164°) in the first growth stage to 3·15 radians (180°) in the last stage (Text-fig. 3C). The increase is reflected in the migration of ribs radially around the margin (Text-fig. 1C). This pattern of radial displacement causes a distinct curvature of the ribs during growth (see Text-fig. 1A, and Discussion section).

Finally, the spiral geometry on the right valve is expressed by a relationship between the angular position (θ) and the radius's logarithm, $\log(r)$ (Text-fig. 2C). The radial expansion rate (σ) is the slope of the line, and this defines the whorl expansion rate (W), according to $W = e^{2\pi\sigma}$ (McGhee 1980). A linear θ–$\log(r)$ relationship, indicates that the spiral is isometric, while a non-linear relationship, as for *P. vogdesi*, indicates allometric whorl expansion. In *P. vogdesi*, the radial expansion rate gradually decreases during growth, meaning that the more flattened juvenile shell becomes more vaulted with increasing size (Text-fig. 3D). The allometry is measured by a second-order regression equation of the form $\log(r) = \sigma_0 + \sigma_1\theta + \sigma_2\theta^2$, where σ_1 is the slope of the line at $\theta = 0$, and σ_2 is related to the curvature. If σ_2 is negative (as in the *P. vogdesi* specimen, $\sigma_2 = -0{\cdot}351$), the function is convex upwards, indicating a decreasing radial expansion rate with increasing size. The radial expansion rate at the time of the last growth stage is given by the slope of the line at $\theta = 0$, which is $\sigma_1 = 0{\cdot}158$.

The θ–$\log(r)$ data are transformed in subsequent analyses (see Results) by considering only the data in the last 60° of the spiral (Text-fig. 3E–F) and transforming these data so that the angles are positive, starting with zero at an angle of $-60°$. The purpose of this transformation is to ensure that comparable data sets are analysed in different *Pecten* specimens (in many flattened species, the spiral data are reliable only for about the last 60° of the spiral), and so that the regression analysis gives the radial expansion rate of an early growth stage (at $\sigma_1 = 60°$) and the trend thereafter (σ_2).

METHODS

The valves of seven named and two unidentified *Pecten* species (Table 1) were measured either by: (1) measurements with callipers and subsequent calculations to transform the data into x,y,z, space; (2) making camera lucida drawings of the valves and subsequently digitizing the data; or

TABLE 1. *Pecten* species used in the analysis.

Species	Number of specimens
P. fumatus	4
P. jacobeus	2
P. laqueatus	3
P. maximus	5
P. meridionalis	4
P. spinulosum	1
P. vogdesi	2
P. sp. (unidentified)	2
Total specimens	23

(3) digitizing directly from a video imaging system. Digitized points represent the intersections of ribs and growth lines on the flattened left valve, and the outline of the spiral on the convex right valve. On the flattened valve, only certain ribs and growth lines were chosen for measurement, in order to expedite the analysis. The posterior- and anterior-most 'ribs' are close to, but not on, the edge of the shell. The hinge line was approximately horizontal when the shells were digitized; thus, the x-axis is approximately parallel to the hinge, and the y-axis approximately perpendicular to the hinge.

After digitizing, the following steps were performed by computer on data for the flattened left valve.

1. Circles were fitted to each aperture (apex was not included) by a non-linear regression technique which found the best-fit centre (x,y position) and radius (see Appendix). The radius was taken as a measure of aperture size.
2. An ellipse was fitted to each aperture by linear regression (see Appendix) using the circle centre found in step 1. Note that the axes of the ellipse are parallel to the x and y axes (approximately parallel and perpendicular to the hinge line). This orientation is arbitrary; a more sophisticated computer algorithm would find the best-fit orientations of the axes.
3. The following parameters were calculated for successive growth stages in each specimen: (*a*) aspect ratio of the fitted ellipse (a/b; Text-fig. 2A); (*b*) the distance of the ellipse centre from the apex along the y-axis (y_c; Text-fig. 2A); and (*c*) the ventral sector angle of the ellipse subtended by the shell margin (Text-fig. 2B).

The spiral geometry of the convex right valve was analysed by digitizing the spiral outline and calculating the distance (r) and angular position (θ) of a series of points on the spiral (Text-fig. 2C).

RESULTS

Text-figures 4–6 show selected examples of the data for three *Pecten* specimens (also see Text-fig. 1). The illustrations show that ellipses fit the geometry of the aperture very well, and in most cases the aperture is very nearly circular ($a/b \approx 1$; see below). Almost all specimens exhibit allometric growth, recorded as ontogenetic variations in the growth parameters.

Ontogenetic variation in the flattened valve

Ontogenetic trends in the parameters for the flattened left valve (aspect ratio, aperture position, and ventral sector angle) are plotted in Text-figures 7–9 (see the example, Text-fig. 3). In order to summarize the ontogenetic variation, regression lines were fitted to the trends in each parameter (23 regression lines per parameter). The regression lines (reduced major axis) give the slope of each trend and the value of the parameter at an aperture radius of 2 cm. This value was chosen because all data sets have values corresponding to this shell size (or close to it), and hence the value is within the range of the data.

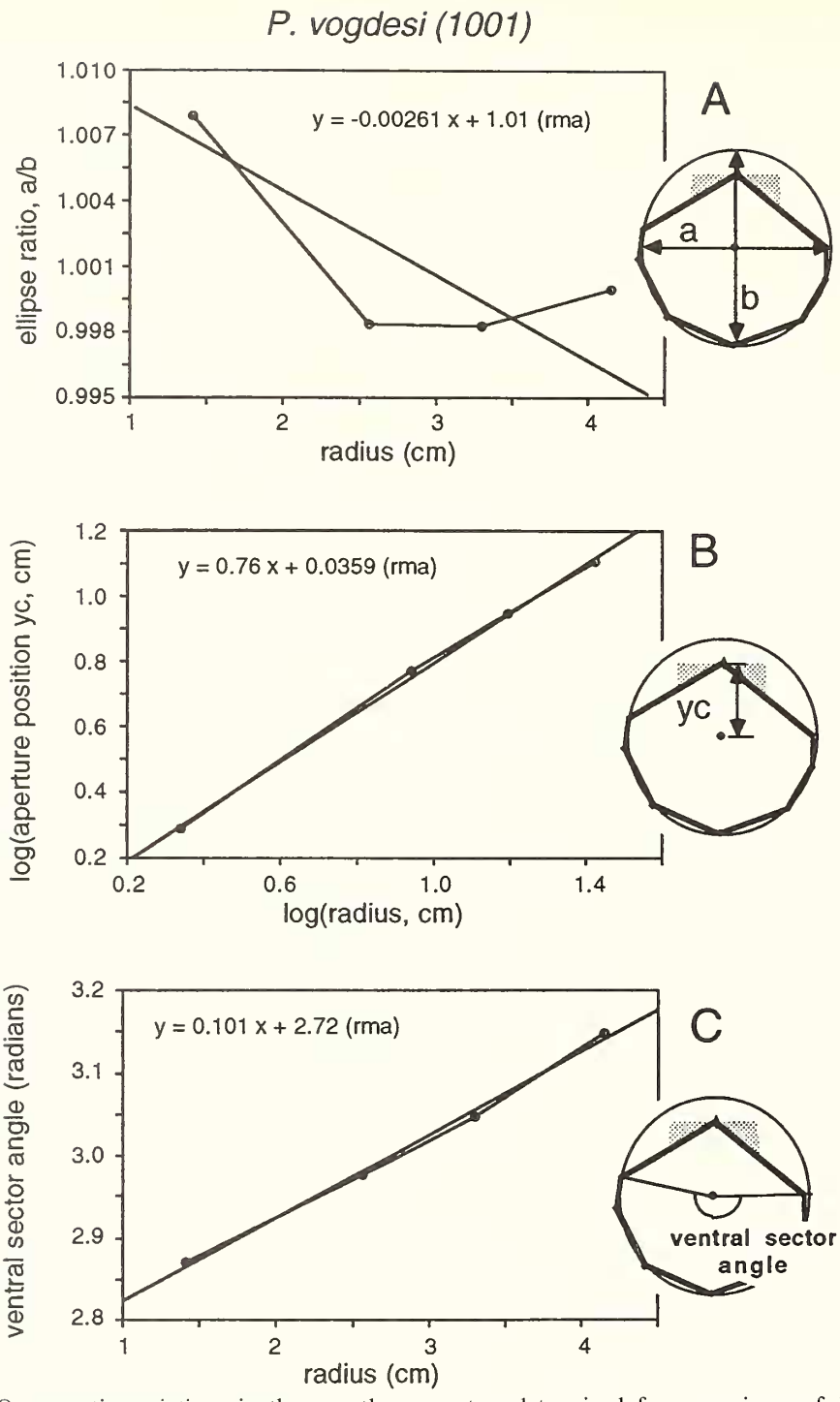

TEXT-FIG. 3. Ontogenetic variations in the growth parameters determined for a specimen of *P. vogdesi*. A, the aspect ratio of the shell margin varies with aperture size (radius). The trend is estimated by a reduced major axis regression. B, the apex–aperture distance increases with increasing size. A reduced major axis regression for the log–log relationship gives a slope less than one, indicating negative allometric growth in this parameter, i.e. the apex and aperture migrate relatively towards each other during growth. C, the ventral

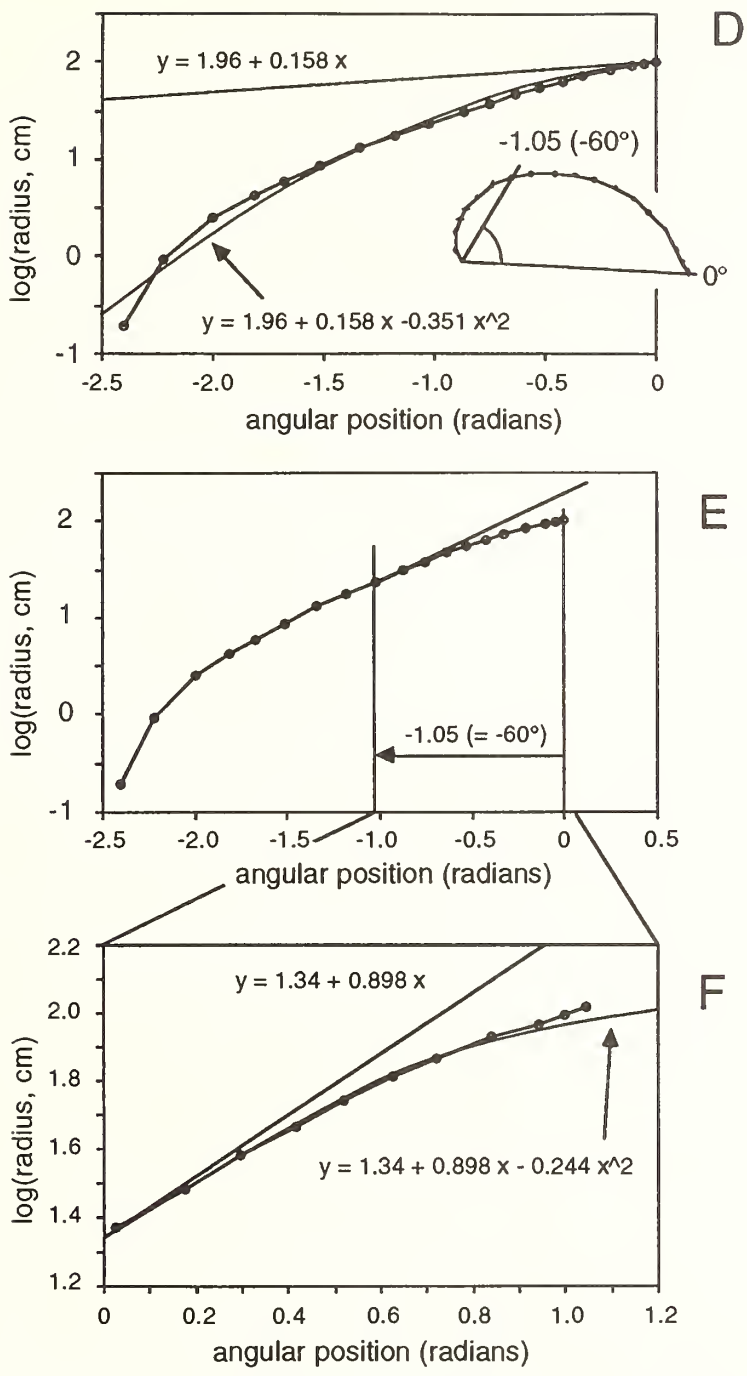

sector angle increases slightly with size. D, the radial expansion rate of the spiral is estimated from a regression of $\log(r)$ against θ, for data from the convex right valve. The relationship is curvilinear (convex upwards, $\sigma_2 = -0{\cdot}351$) indicating that the radial expansion rate decreases during growth. E, in loosely coiled shells, data are reliable only for the last 60° of the spiral, and the regression is performed on this part of the data. F, the data in E are transformed so that $-60°$ is equal to zero.

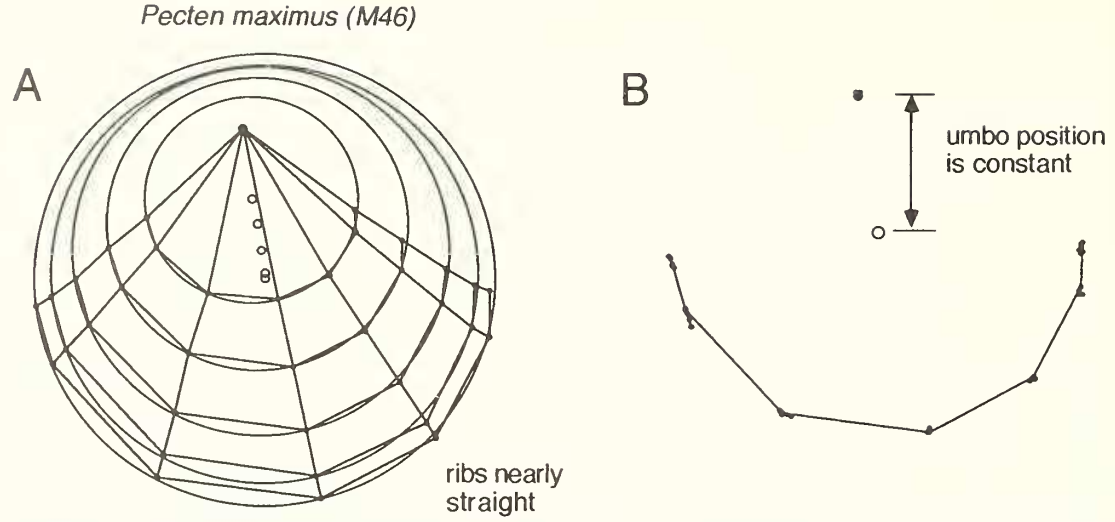

TEXT-FIG. 4. Results of the analysis for a specimen of *P. maximus* (specimen M46). A, the digitized outlines of growth stages, and ribs, with ellipses fitted to the shell margin. B, successive apertures are rescaled to the same size, and registered to a common origin. The diagram shows the relative positions of the apex (in this case it is constant during growth), and of ribs. The outline is the last growth stage.

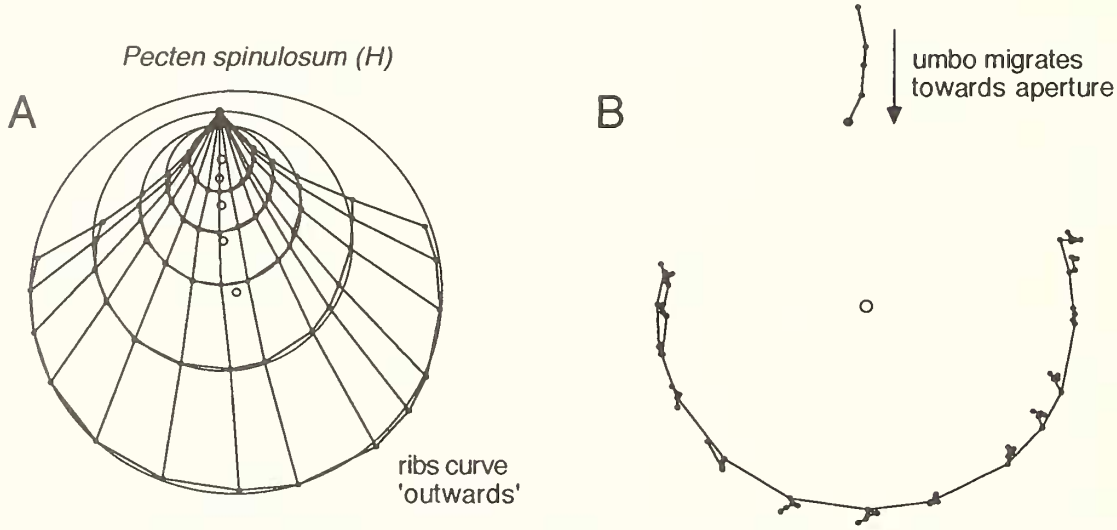

TEXT-FIG. 5. *Pecten spinulosum* (specimen H). See Text-fig. 4 caption for details. This specimen is unusual for *Pecten*. The aperture is located distally from the apex in early growth stages, and the aperture migrates rapidly towards the apex, in a relative sense, during growth, resulting in strongly arcuate ribs.

The distribution of regression intercepts (at $r = 2$ cm) and the slopes for each parameter are plotted in the histograms in Text-figures 10–12. Thus, the mean value of the aspect ratio at $r = 2$ cm is 1·006 (Text-fig. 10A), and the mean trend is zero (Text-fig. 10B). The mean trend is indicated by the heavy shaded line in Text-figure 7. The mean position of the aperture centre at $r = 2$ cm is 15·6 mm (Text-fig. 11A), and the log–log relationship gives a mean slope of 0·89 (Text-

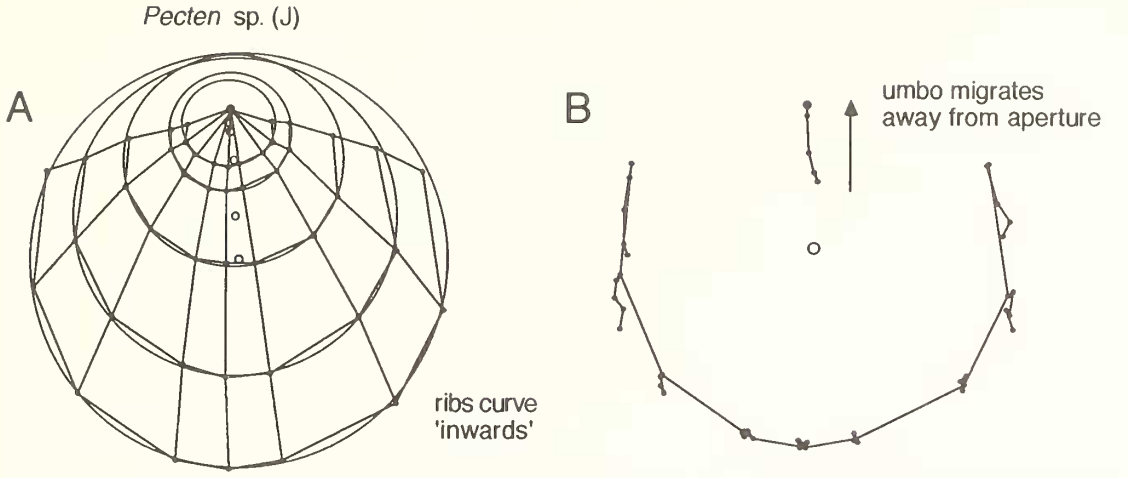

TEXT-FIG. 6. A large *Pecten* (specimen J). See Text-fig. 4 caption for details. The specimen is unusual. The aperture is located quite close to the apex in early growth stages, but migrates rapidly away from the aperture, in a relative sense, during growth, resulting in ribs which are curved 'inwards'. Inward curving ribs are rare in *Pecten*.

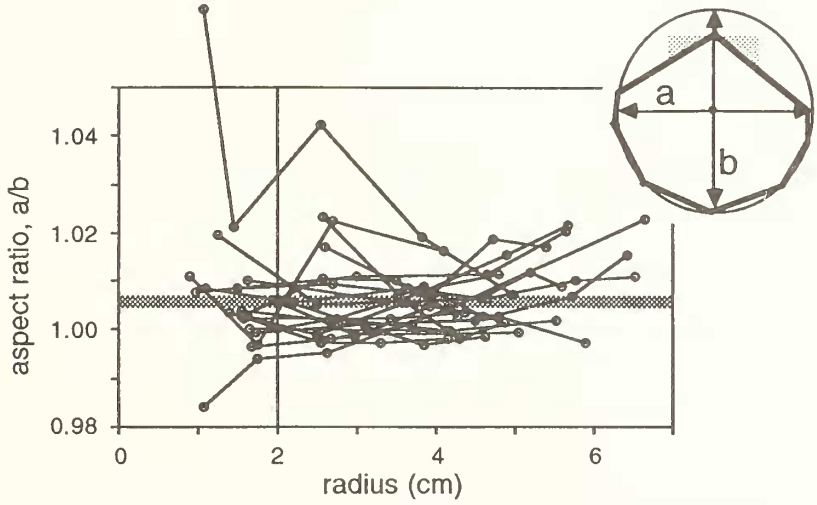

TEXT-FIG. 7. Trends in the aspect ratio of the aperture ellipse a/b, as a function of aperture size r, for the 23 specimens in the analysis. The mean value of the aspect ratio at a radius $r = 2$ cm is 1·006 and the mean trend is zero, as determined by regression analysis on each of the individual specimens (see Text-fig. 10).

fig. 11B). This trend is indicated by the heavy line in Text-figure 8. A slope of 1 represents isometric growth; therefore on average in *Pecten*, the aperture migration rate is negatively allometric, as discussed for the specimen of *P. vogdesi* (Text-figs 1, 3). Finally, the mean value of the ventral sector angle at $r = 2$ cm is 3·05 radians (175°) (Text-fig. 12A), and the mean slope of the trend is 0·058 radians/cm (Text-fig. 12B). The trend is indicated by the heavy line in Text-figure 9. Thus on average in *Pecten*, the arc length of the shell margin increases during growth (by about 0·23 radians, or 13°, for a radius increase of 4 cm) (also see *P. vogdesi* example, Text-figs 1, 3).

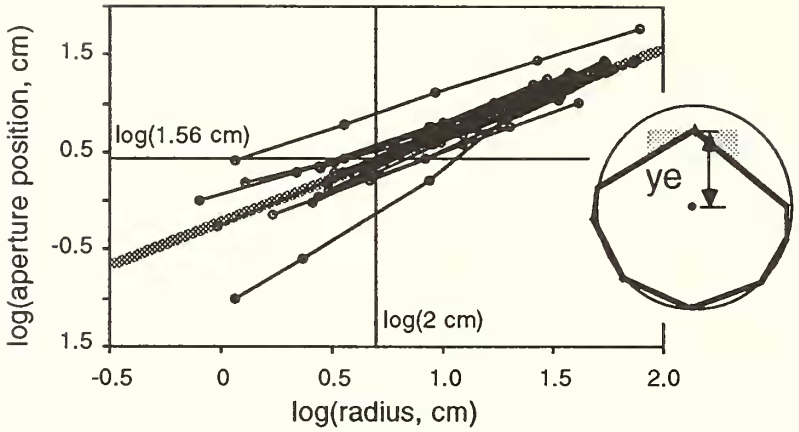

TEXT-FIG. 8. Trends in the relative aperture–apex position, y_c, as a function of aperture size r, for the 23 specimens in the analysis, expressed as a log–log relationship. The mean value of y_c is 1·56 cm at a radius $r = 2$ cm. The mean slope of the relationship is 0·885 indicating that on average, in *Pecten*, the aperture migrates relatively towards the apex during growth (also see Text-fig. 11).

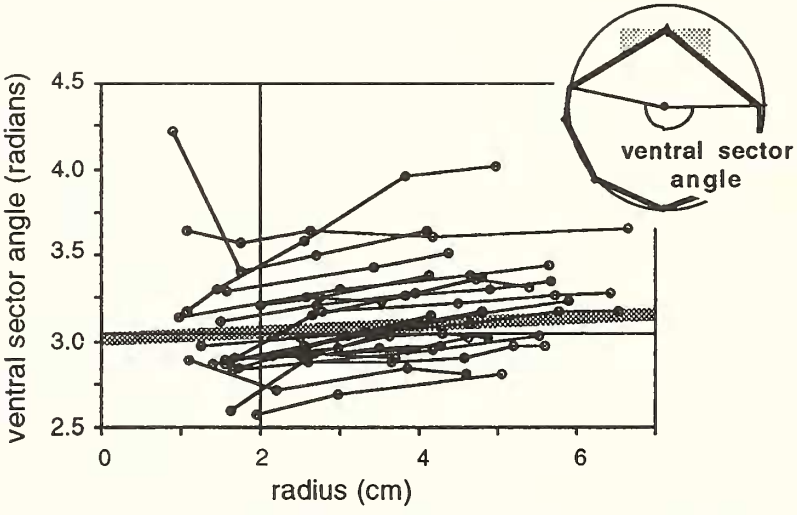

TEXT-FIG. 9. Trends in the ventral sector angle as a function of aperture size r. The mean value of the ventral sector angle at a size $r = 2$ cm is 3·05 and mean trend is for the angle to increase slightly with size (also see Text-fig. 12).

Ontogenetic variation in the spiralled valve

Ontogenetic variation in the spiralled valve of *Pecten* is reflected in variations in the radial expansion rate with growth, i.e. the slope of the trend of $\log(r)$ against angular position (θ) for points on the spiral (Text-fig. 13A). The curvilinear trends for *Pecten* indicate that the radial expansion rate changes during ontogeny, as discussed for *P. vogdesi* (Text-figs 1, 3). The data suggest two growth phases for *Pecten*; a juvenile stage characterized by rapid expansion of the shell (large slopes, high radial expansion rates), and a later stage characterized by slower expansion and

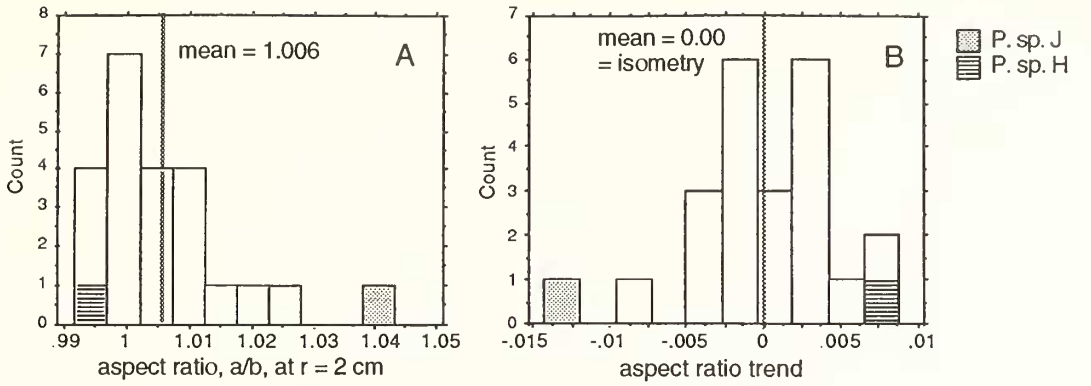

TEXT-FIG. 10. The trend of aspect ratio with increasing size (Text-fig. 7) is analysed by reduced major axis regression, giving the distribution of values for the aspect ratio at $r = 2$ cm, and the slope of the trend. A, the mean aspect ratio is $1{\cdot}006 \pm 0{\cdot}005$ ($p = 0{\cdot}05$). B, the mean aspect ratio trend is $0{\cdot}000 \pm 0{\cdot}002$ ($p = 0{\cdot}05$). Two specimens are unusual, *P.* sp. H and *P.* sp. J (see Text-figs 5 and 6 respectively).

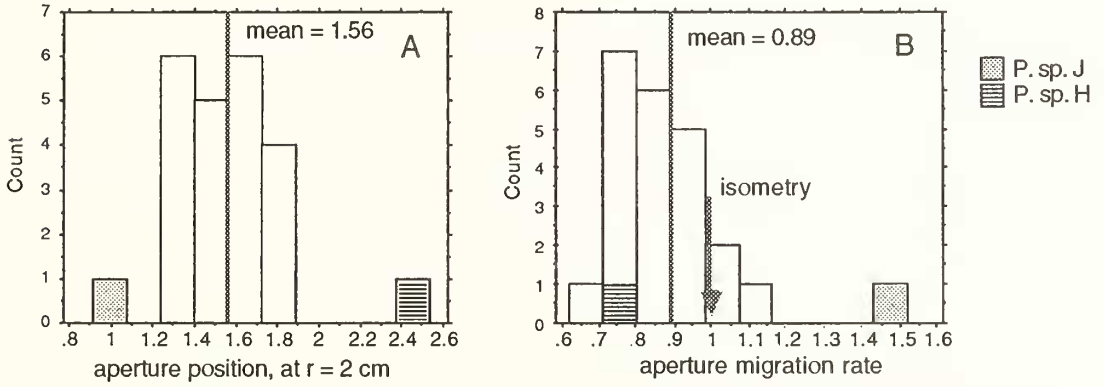

TEXT-FIG. 11. The trend of aperture position, y_c, with increasing size, is analysed by reduced major axis regression, applied to the log–log relationship (Text-fig. 8), giving the distribution of values for the aperture position at $r = 2$ cm, and the slope of the log–log trend (the aperture migration rate). A, the mean aperture position is $1{\cdot}56 \pm 0{\cdot}123$ cm ($p = 0{\cdot}05$). B, the mean aperture migration rate is $0{\cdot}885 \pm 0{\cdot}077$ ($p = 0{\cdot}05$).

doming of the shell. The juvenile phase probably corresponds roughly to the first year of growth (the flattened left valve is slightly concave during this early growth stage).

In this analysis only allometries occurring in the adult stage were considered. The data were edited and all points on the spiral greater than 60° from the last aperture position were removed. This procedure was necessary because in many *Pecten* species the radial expansion rate is high and spiral data exist only in the 0 to 60° range (e.g. see loosely coiled spiral in Text-fig. 13). After removing all angles greater than 60°, all angles were converted to positive values by adding 1·047 radians (60°) to each, giving the new data set in Text-figure 13B. Ontogenetic variation was recorded by a second-order least-squares regression, of the form $\log(r) = \sigma_0 + \sigma_1\theta + \sigma_2\theta^2$, where σ_1 is the slope of the line at $\theta = 0$, and σ_2 gives the curvature (see p. 850). If σ_2 is negative, the function is convex upwards (as in the *P. vogdesi* specimen, Text-fig. 3D), and the radial expansion rate decreases with increasing size. If σ_2 is positive the reverse is true. The mean slope of $\sigma = 1{\cdot}33$ (Text-fig. 14A) gives the mean whorl expansion rate of the specimens measured ($W = e^{2\pi\sigma} = 4{\cdot}26 \times 10^3$).

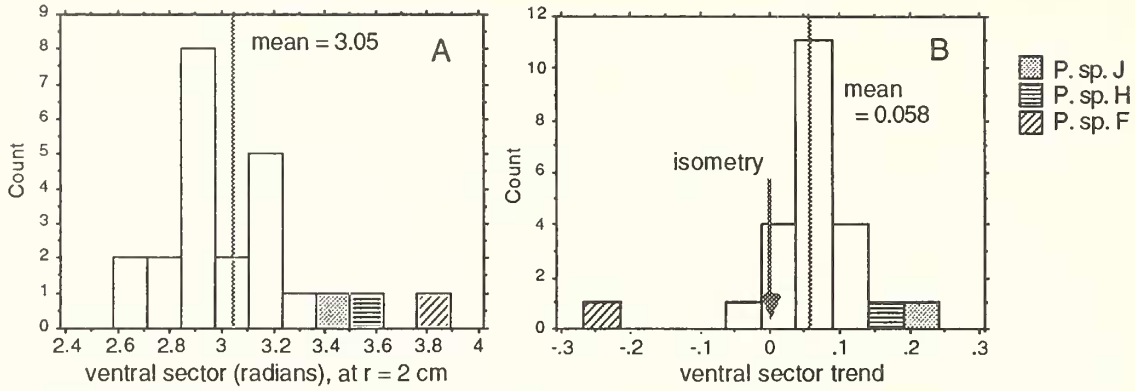

TEXT-FIG. 12. The trend of the ventral sector angle with increasing size (Text-fig. 9) is analysed by reduced major axis regression, giving the distribution of values for the ventral sector angle at $r = 2$ cm, and the slope of the trend. A, the mean ventral sector angle is $3{\cdot}05 \pm 0{\cdot}123$ radians ($p = 0{\cdot}05$). B, the mean ventral sector angle trend is $0{\cdot}058 \pm 0{\cdot}038$ radians/cm ($p = 0{\cdot}05$).

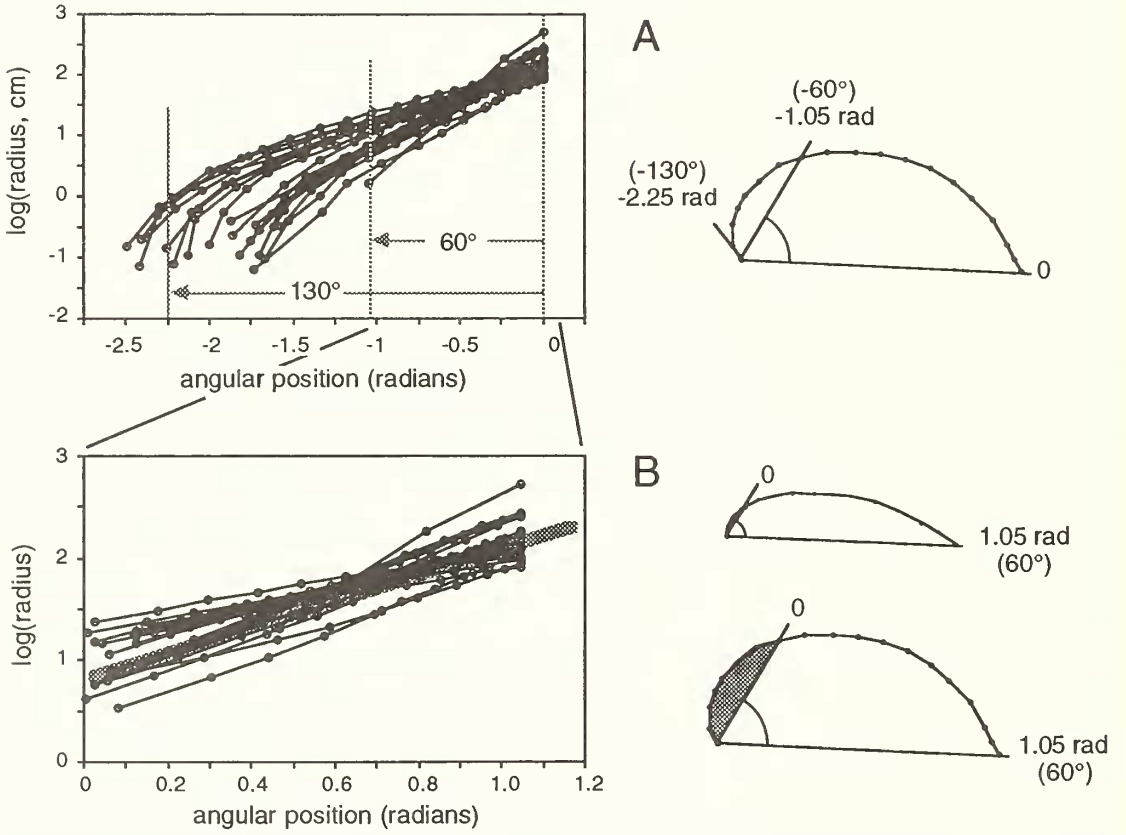

TEXT-FIG. 13. The radial expansion rate of the convex right valve is equal to the slope of the relationship between $\log(r)$ against θ. A, *Pecten* shells show high radial expansion rates early in ontogeny, with rates decreasing with increasing size. B, the data are edited to exclude all values of θ greater than 60° from the last growth stage, and then transformed so that the last growth stage is at +60°. Regression analysis (see Text-fig. 14) gives the radial expansion rate at the 60° position, and the curvature of the relationship defines the extent of allometry in the radial expansion rate during the latter stages of growth.

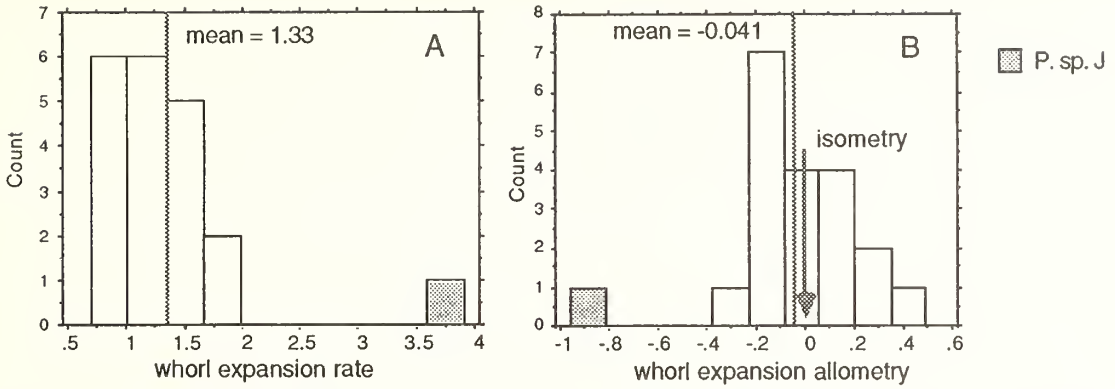

TEXT-FIG. 14. The trend of the radial expansion rate with increasing size is analysed by a second-order least-squares regression, applied to the log(r) vs. θ relationship (Text-fig. 13), giving the distribution of values for the radial expansion rate, and the extent of allometry in the radial expansion rate. A, the mean radial expansion rate is $1{\cdot}33 \pm 0{\cdot}311$ ($p = 0{\cdot}05$). B, the mean radial expansion rate allometry is $-0{\cdot}041 \pm 0{\cdot}131$ ($p = 0{\cdot}05$).

The mean curvature of $\sigma_2 = -0{\cdot}041$ (Text-fig. 14B), is not significantly different from zero, suggesting that on average the *Pecten* spiral is isometric during the last 60° arc of growth.

The structure of ontogenetic variation

The mean ontogenetic trends in the shape parameters reveal the average shell morphology in *Pecten* (see Discussion). But the data also permit a more detailed analysis of how the shape parameters might be inter-related. For example, is the aspect ratio, or its ontogenetic trend, in a given specimen related to the position of the aperture, or its migration rate away from the shell apex? A non-parametric Spearman rank correlation matrix shows the relationships between the growth parameters in the 23 specimens (Table 2). Interestingly, specimens which often appear as outliers (F, J, and H) tend to confirm the general trends, and greatly extend the range of observations.

The strongest correlations ($p < 0{\cdot}005$) are inverse relationships between the starting value of a

TABLE 2. A non-parametric correlation matrix relating the values of the ontogenetic parameters and their patterns of ontogenetic variation (Spearman's rank correlation coefficient). Parameters: $b0_{a/b}$, value of the aspect ratio at $r = 2$ cm; $b1_{a/b}$, trend of the aspect ratio with increasing radius (units: cm^{-1}); $b0_{yc}$, position of aperture centre at $r = 2$ cm (units: cm); $b1_{yc}$, trend of the aperture centre position with increasing radius; slope of log–log relationship; $b0_{vsec}$, ventral sector angle at $r = 2$ cm (units: radians); $b1_{vsec}$, trend in the ventral sector angle with increasing radius (units: radians/cm); $b1\sigma$, radial expression rate at $\theta = -60°$; $b2\sigma$, trend in the radial expansion rate.

	$b0_{a/b}$	$b1_{a/b}$	$b0_{yc}$	$b1_{yc}$	$b0_{vsec}$	b_{vsec}	$b1\sigma$	$b2\sigma$
$b0_{a/b}$	1·0							
$b1_{a/b}$	−0·599**	1·0						
$b0_{yc}$	−0·417	0·363	1·0					
$b1_{yc}$	0·431	−0·191	−0·687**	1·0				
$b0_{vsec}$	0·133	−0·270	−0·296	0·062	1·0			
$b1_{vsec}$	−0·037	−0·318	−0·389	0·405	−0·070	1·0		
$b1\sigma$	0·302	−0·144	−0·338	0·738**	0·235	−0·123	1·0	
$b2\sigma$	−0·026	0·056	0·071	0·206	0·131	−0·032	−0·057[1]	1·0

** $p < 0{\cdot}005$; [1] The Pearson correlation coefficient is $-0{\cdot}68$ ($p < 0{\cdot}005$).

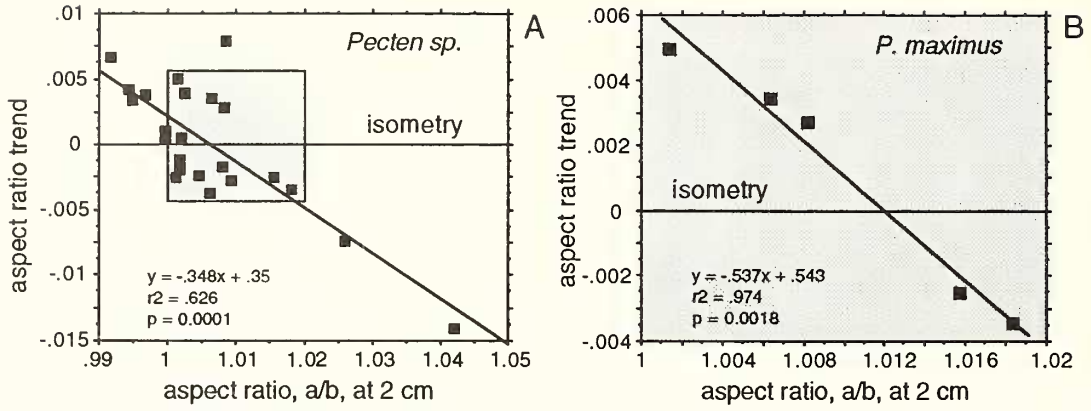

TEXT-FIG. 15. A, an inverse relationship exists between the initial value of the aspect ratio of the shell margin and its trend with size. When the initial aspect ratio is small, the ratio increases with size, whereas when the initial aspect ratio is large, the ratio decreases with size. Shells isometric in the aspect ratio parameter fall on the horizontal line. B, the trend is more pronounced at the intraspecific level (data for *P. maximus*).

parameter and its trend. These inverse relationships occur in at least two, and probably three, of the four growth parameters: aspect ratio, aperture position, and radial expansion rate (but not ventral sector angle). The relationship between the aspect ratio and its trend (Text-fig. 15) shows that apertures which are initially elongate (high a/b) become less so during growth (trend < 0), and those that are narrow (low a/b) become more elongate during growth (trend > 0). The relationship occurs interspecifically (Text-fig. 15A) but is even more pronounced in the intraspecific sample of *P. maximus* (chosen because this species has the largest sample size; $n = 5$) (Text-fig. 15B). Two specimens stand out, an unidentified *Pecten* sp. (*P.* sp. J) and a specimen of *P. spinulosum* (*P.* sp. H). These specimens are highlighted on the histogram (Text-fig. 10), and represent the highest and lowest values of the aspect ratio.

The position of the aperture shows a similar inverse relationship (Text-fig. 16). When the shell margin is initially farther away from the apex (aperture position is large), the tendency is to migrate

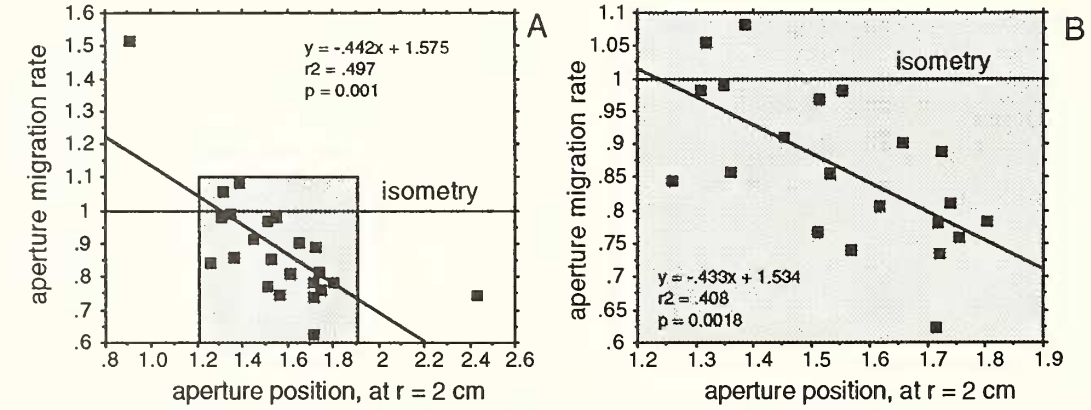

TEXT-FIG. 16. A, an inverse relationship exists between the initial value of the aperture position and its trend with size. When the initial value is small, the aperture position migrates relatively away from the apex with increasing size, whereas when the initial value is large, the aperture migrates relatively towards the apex with increasing size. Shells isometric in the aperture position fall on the horizontal line. B, the trend is illustrated after removing the unusual specimens of *P.* sp. H and *P.* sp. J (see Text-figs 5 and 6 respectively).

relatively towards the apex during growth (small migration rate), but when the shell margin is initially close to the apex (aperture position is small), the tendency is to migrate relatively away from the apex during growth (large migration rate). Note that the trend in aperture position is relatively towards the apex in most specimens (migration rate < 1), but the magnitude of the trend is inversely proportional to the starting value. Interestingly, *P.* sp. J stands out once again, with an aperture very close to the apex at small sizes, but a tendency to migrate rapidly away from the aperture with increasing size. This is the one specimen that shows significantly positive allometry in the migration rate, and the ribs are curved inwards rather than outwards as in most *Pecten* specimens. The inverse relationship remains, even after removing the unusual specimens *P.* sp. J and *P.* sp. H (Text-fig. 16B).

Finally, the radial expression rate shows a probable inverse relationship between its starting value and its trend. The trend is highly significant in the interspecific sample of *P. maximus* (Text-fig. 17B) and is suggested (though not statistically confirmed) in the intraspecific sample (Text-fig. 17A). Thus, when the radial expansion rate is initially high, its value appears to decrease during ontogeny (negative allometry), but when the expansion rate is initially low, it tends to increase during ontogeny (positive allometry).

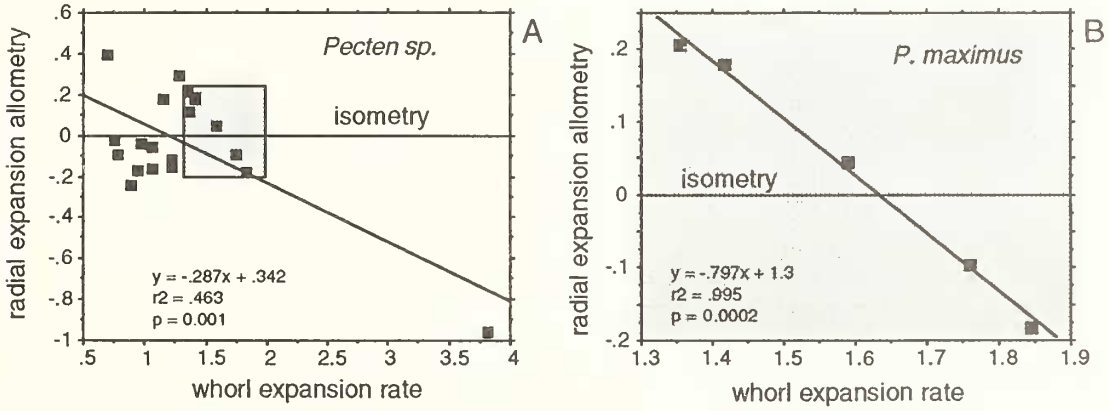

TEXT-FIG. 17. A, an inverse relationship exists between the initial value of the radial expansion rate and its trend with size. When the initial value is small, the radial expansion rate increases with size, whereas when the initial value is large, the radial expansion rate decreases with size. Shells isometric in the radial expansion rate fall on the horizontal line. B, the trend is more pronounced at the intra-specific level (data for *P. maximus*).

One significant correlation occurs between the growth parameters. The radial expansion rate on the convex valve is positively correlated with the aperture migration rate on the flattened valve (Text-fig. 18). That is, large radial expansion rates correlate strongly with large aperture migration rates.

DISCUSSION

The analysis of *Pecten* shell geometry is based on a model where the shell margin is a sector of an ellipse and where the margin is expanding and migrating away from the shell apex (and rotating in the convex valve). Measurements of 23 specimens show the basic geometry of the shell, and how the geometry varies during growth. Correlations between growth parameters define the distribution of shell geometries observed within the genus.

One of the interesting results of the analysis is that the shell margin in *Pecten* is basically circular (aspect ratio close to 1), extending along an arc of about 175°. The arc length of the shell margin generally increases slightly during growth, but the circular shape of the margin is conserved

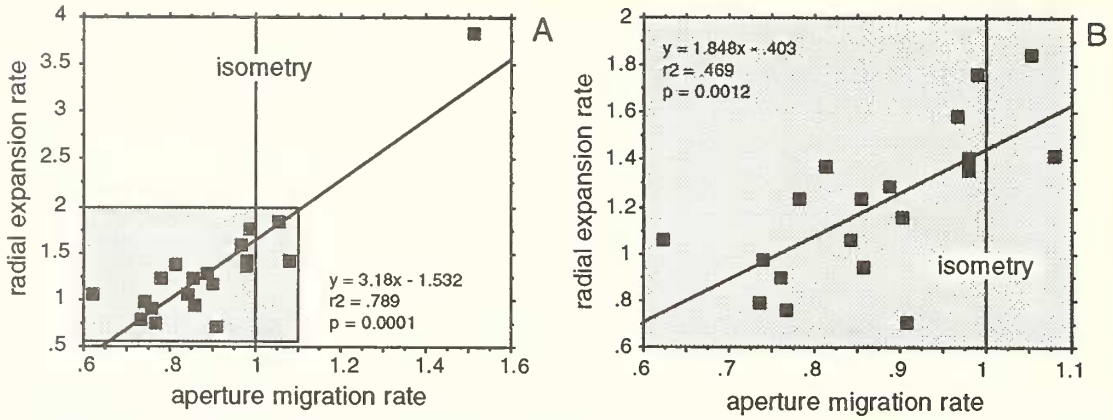

TEXT-FIG. 18. A, a direct relationship exists between the radial expansion rate in the convex right valve, and the rate of aperture migration away from the apex in the flattened left vale. When the initial radial expansion rate is small, the aperture migrates, in a relative sense, rapidly towards the apex during growth, whereas when the initial radial expansion rate is large, the migration rate of the aperture is reduced. B, the same data but with the *P.* sp. J specimen removed.

(variations in the aspect ratio during growth are small, within the range 0·995 to 1·005). The circular geometry is an apparently conservative feature of pectinid growth, perhaps representing a mechanical constraint on the mantle tissues, such as fluid tensions within the mantle (the 'pneu principle': see Savazzi 1990).

The most pronounced variations in *Pecten* morphology are related to: (1) the position of the shell margin relative to the shell apex; (2) the radial displacement of ribs around the margin; and (3) the radial expansion rate of the convex right valve. The mean *Pecten* shape is illustrated by a simulation (Text-fig. 19A) with inputs of the mean values of the parameters and their variation with size (see Text-figs 7–14). On average, the aperture centre (defined as the centre of a best-fit ellipse to the margin) is less than one aperture radius from the shell apex, with the relative distance decreasing with increasing shell size.

Allometric rib curvature in *Pecten* is a result of both (1) radial displacement of ribs around the margin, and (2) relative migration of the aperture towards the shell apex (Text-fig. 19B). The relative contributions of these two factors is observed in computer simulations, showing a shell with allometry only in the aperture migration rate (Text-fig. 19C) and a shell with allometry only in the ventral sector angle (Text-fig. 19D). These allometries combine to produce the curvature of the ribs in the mean *Pecten* shell form. In an isometric shell the ribs would be straight (Text-fig. 19E).

Perhaps the most significant and unexpected result of the analysis is the pattern of covariation observed in the growth parameters. Inverse relationships are strong between the starting value of a parameter and its trend with size. Thus, the aspect ratio increases with size when the initial value is small, and vice versa. The aperture migration rate is greater when the initial aperture position is near the shell apex, and vice versa. The radial expansion rate increases when its initial value is small, and vice versa. The effects of these inverse relationships on shell morphology are assessed by the simulations in Text-figure 20, showing a range of possible combinations of aperture position and migration rate (applies to the flat valves), and radial expansion rate and the trend in radial expansion rate (applies to the convex valves) (variations in the aspect ratio of the margin are small and are not considered below). The preceding regression analysis defined the following relationships between the parameters:

$$dy/dr = 1{\cdot}58 - 0{\cdot}442\,y \quad \text{(see Text-fig. 16)} \tag{1}$$

$$d\sigma/dr = 0{\cdot}342 - 0{\cdot}287\,\sigma \quad \text{(see Text-fig. 17)} \tag{2}$$

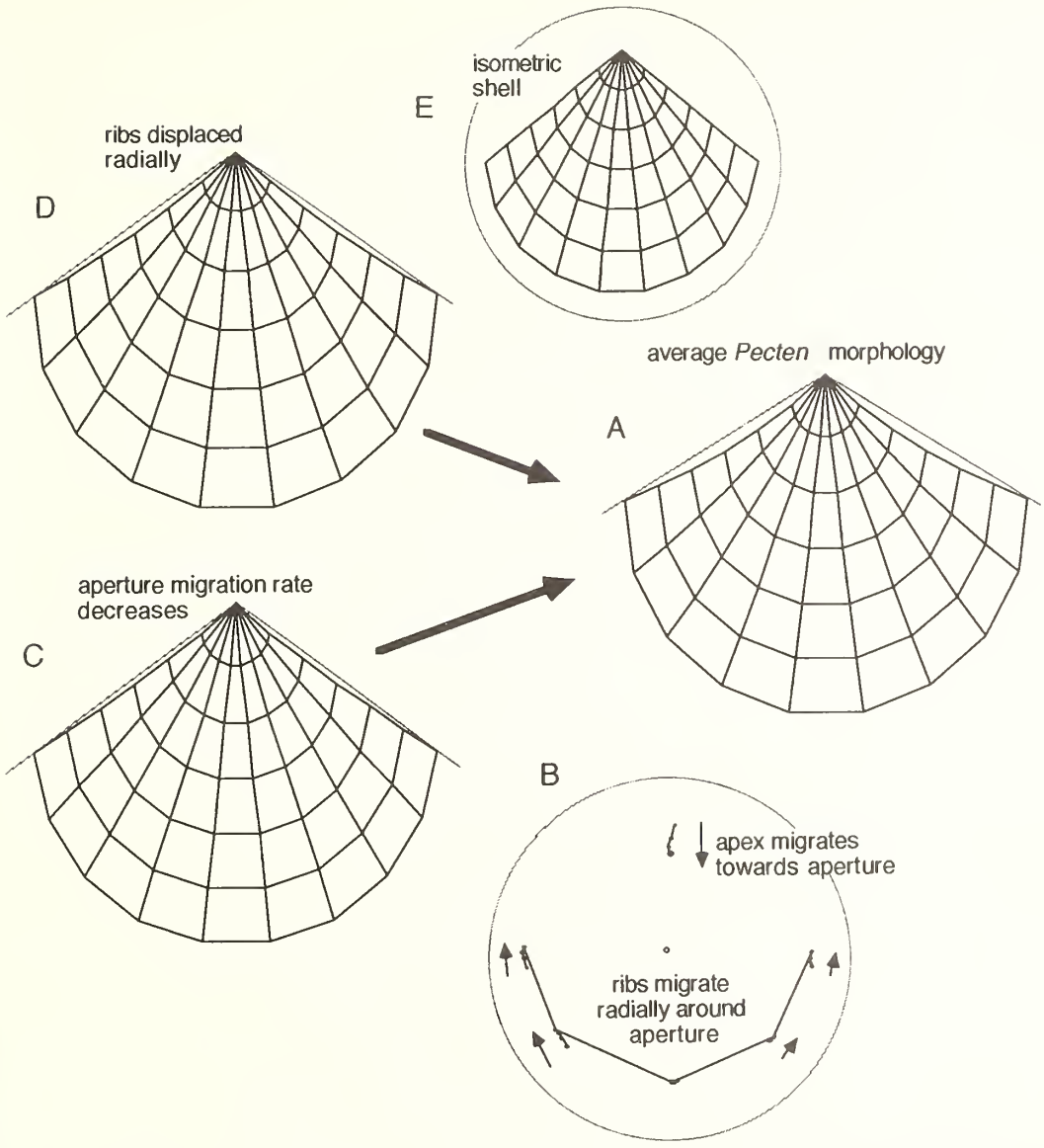

TEXT-FIG. 19. Simulation of *Pecten* shell geometries (flattened left valve). A, the mean *Pecten* geometry. The aperture is circular, the ventral sector angle increases at a rate of 0·058 radians/cm from a value of 3·05 radians at $r = 2$ cm. The aperture position increases as $r^{0.89}$, from an initial value of 1·56 at $r = 2$ cm. B, rib curvature is due to relative increases in the ventral sector angle and relative decreases in the distance of the aperture from the apex during growth. C, observed allometry in *Pecten* due to increases in the ventral sector angle only. D, observed allometry in *Pecten* due to variation in the aperture migration rate only. E, a hypothetical isometric shell with straight ribs.

where y is the aperture position, dy/dr its migration rate, σ is the radial expansion rate and $d\sigma/dr$ its variation with size. These relationships indicate that geometric variation is constrained to a small subset of all possibilities, indicated by the highlighted shell forms (Text-fig. 20). Moreover, the

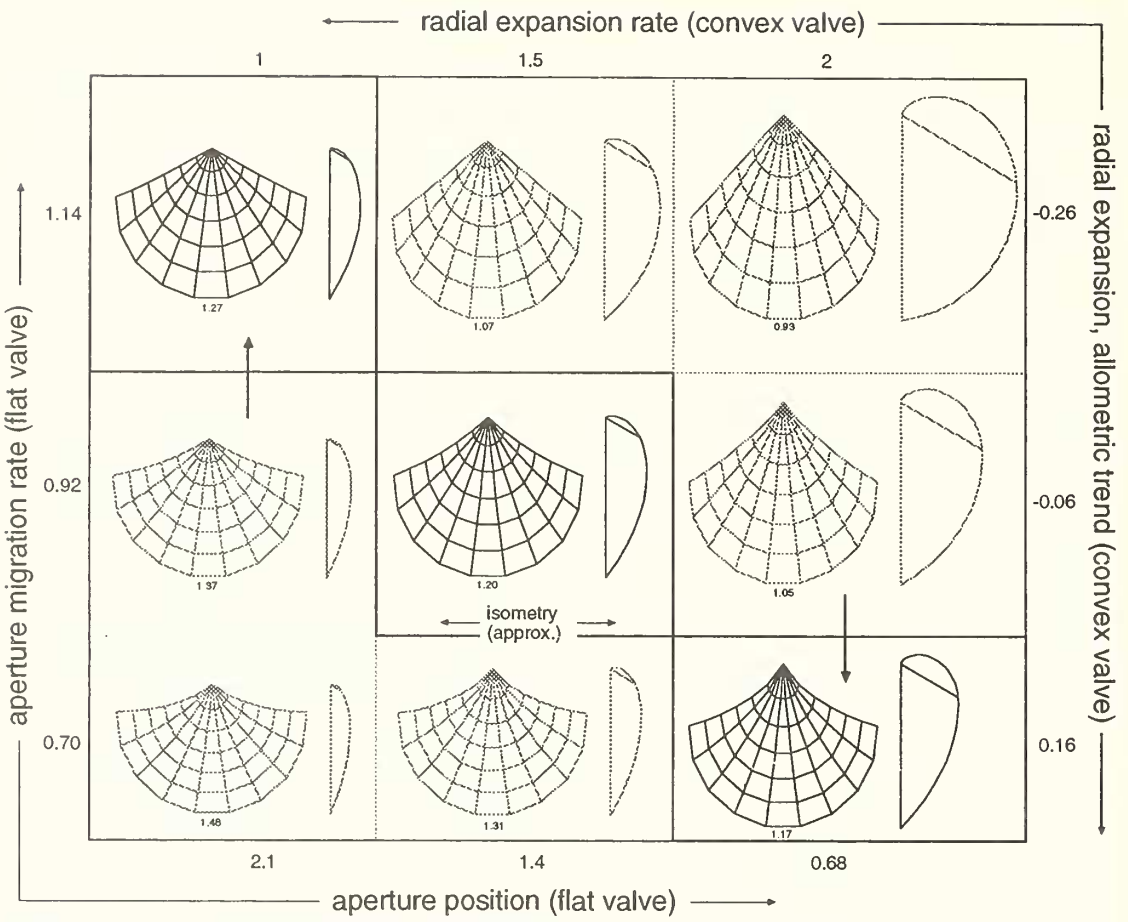

TEXT-FIG. 20. Relationships between growth parameters constrain the variation observed in *Pecten* to a small subset of possible forms, highlighted in black. Shaded figures represent hypothetical forms not present in the sample. The figure shows flat valve parameters: an inverse relationship between aperture position (at $r = 2$ cm) and aperture migration rate, and convex valve parameters: an inverse relationship between the radial expansion rate and allometry in the radial expansion rate. The radial expansion rate and aperture migration rate are directly related, yielding the observed combination of flat valve and convex valve parameters (see text). The geometries on the horizontal shaded line are nearly isometric (aperture migration rate = 1; radial expansion trend = 0), except that there is radial displacement of ribs (increasing ventral sector angle) in all specimens. The diagonal line represents geometries with a length to height ratio of 1·2 (L/H ratios are indicated below each figure). The vertical arrows represent observed directions of ontogenetic variation. Note that the spiral geometry between 60° and the shell apex is slightly modified ($\sigma_{1,i+1} = 1{\cdot}05^{*}\sigma_{1,i}$ for $\Delta\theta = 5°$) to conform to observed shell geometries; the regression analysis did not treat the data in this part of the spiral (unmodified spirals may not converge on the apex).

regression analysis suggests a relationship between the radial expansion rate σ in the convex valve and the aperture migration rate dy/dr in the flattened valve:

$$\sigma = -1{\cdot}53 + 0{\cdot}318\ dy/dr \quad \text{(see Text-fig. 18)} \tag{3}$$

Thus, the highlighted forms in Text-figure 20 represent the observed combinations of left and right valve geometries in *Pecten*. The shaded forms are not present in the sample.

Why is the distribution of *Pecten* geometries constrained to such a small subset of possibilities? Does the distribution reflect adaptive or functional requirements of the organism, or are there perhaps morphogenetic or historical constraints (*sensu* Seilacher 1970) on the morphology of *Pecten*? Inspection of the geometries in Text-figure 20 reveals that the length to height ratio is a conservative feature of pectinid morphology, being on the order of 1·2 in the simulated shell forms. The L/H ratio is apparently maintained by ontogenetic variations, or 'corrections', which modify the shape of the juvenile shell. That is, elongate juvenile shells become taller during growth (upper left, Text-fig. 20), and tall juvenile shells become more elongate (lower right, Text-fig. 20). The absence of ontogenetic corrections would result in a basically isometric geometry (centre left and centre right) (some allometry occurs in all the simulated shells because of radial displacement of ribs around the margin – this value is fixed).

The argument for ontogenetic 'corrections' also applies to variations in the radial expansion rate of the convex valve. For example, a loosely coiled spiral, such as the nearly isometric form in the centre left of Text-figure 20, becomes more vaulted during growth due to an ontogenetic decrease in the radial expansion rate (yielding the form in the upper left), and an initially vaulted shell, such as the form in the centre right of Text-figure 20, becomes more loosely coiled (radial expansion rate increases; see lower right).

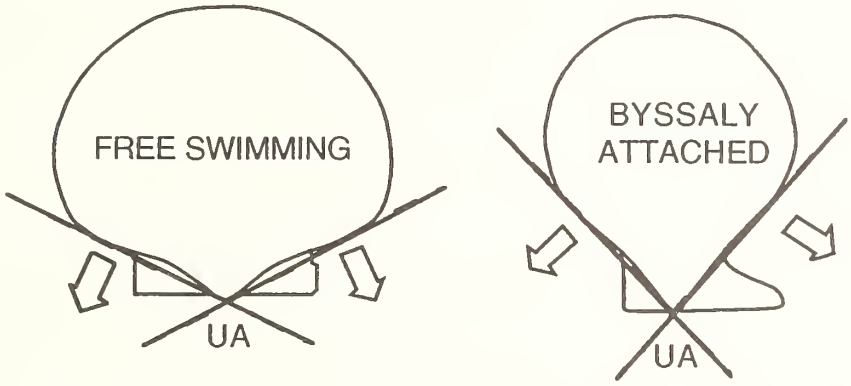

TEXT-FIG. 21. Shell outlines of pectinids with small and large umbonal angles (UA). Shells with large umbonal angles may be more effective swimmers because of the orientation of the dorsally directed jets (large arrows) in these shells (after Stanley 1970, text-fig. 14).

These patterns of ontogenetic variation or 'correction' result in adult *Pecten* shell morphologies with characteristic L/H and L/W ratios. One possible cause for these characteristic dimensions is related to the swimming behaviour of scallops. Stanley (1970), for example, noted that swimming is enhanced by broad shell outlines with large umbonal angles, a shape which permits the dorsally directed jets necessary for swimming. Dorsally directed jets would be difficult in the shell forms in the upper right of Text-figure 20. Forms in the lower left of Text-figure 20, on the other hand, might be functionally deficient for swimming because of their relative shortness which would effectively reduce the internal volume of the shell cavity and hence the water available for propulsion.

The evolutionary and developmental origins of morphological variation in *Pecten* remain problematical. Possibilities include: (1) that evolution has selected for a dynamic, morphogenetic programme, whereby intrinsic juvenile variability is channelled towards a genetically determined, functional adult; or (2) that selection is acting on *Pecten* populations to preserve morphologies which are functionally fit. Answers to these questions will require further analysis of the covariation patterns in both Recent, and fossil populations of *Pecten*.

In summary, the analysis of ontogenetic variation in *Pecten* reveals the intricacies of growth within the genus. The observed patterns of ontogenetic variation are most readily explained in terms

of morphogenetic or functional mechanisms which cause convergence towards a particular morphology. The present study it is hoped will assist in evaluating morphogenetic, functional, and historical arguments for the origin and evolution of growth patterns not only in *Pecten*, but more generally in molluscs.

Acknowledgements. I thank Dolf Seilacher and Wolf Reif (University of Tübingen), and Alwyn Williams, Gordon Curry, Kazuyoshi Endo, and Derek Walton (University of Glasgow) for stimulating and critical discussions on invertebrate growth. Alan Ansell, Dunstaffnage Marine Laboratories, kindly provided specimens, laboratory space, and assistance. Peter Zügel (University of Tübingen) and Fred Naggs (Natural History Museum, London) assisted in the location of specimens. This research was supported in part by funds to Wolf-Ernst Reif from Sonderforschungsbereich, SFB 230, and in part by a NATO postdoctoral fellowship for research in the Department of Geology and Applied Geology, University of Glasgow and at the Dunstaffnage Marine Laboratories, Oban, Scotland. Research space and use of facilities at the aforementioned institutions are gratefully acknowledged.

REFERENCES

ACKERLY, S. C. 1989. Kinematics of accretionary shell growth, with examples from brachiopods and molluscs. *Paleobiology*, **15**, 147–164.

MCGHEE, G. R. 1980. Shell form in the biconvex articulate Brachiopoda: a geometric analysis. *Paleobiology*, **6**, 57–76.

RAUP, D. M. 1966. Geometric analysis of shell coiling: general problems. *Journal of Paleontology*, **40**, 1178–1190.

SAVAZZI, E. 1990. Biological aspects of theoretical shell morphology. *Lethaia*, **23**, 195–212.

SCHINDEL, D. E. 1990. Unoccupied morphospace and the coiled geometry of gastropods: architectural constraint or geometric covariation? 270–304. *In* ROSS, R. M. and ALLMON, W. D. (eds). *Causes of evolution: a paleontological perspective*. University of Chicago Press, Chicago, 479 pp.

SEILACHER, A. 1970. Arbeitskonzept zur konstruktions-morphologie. *Lethaia*, **3**, 393–396.

SNEDECOR, G. W. and COCHRAN, W. G. 1980. *Statistical methods*. Iowa State University Press, Ames, 507 pp.

STANLEY, S. M. 1970. Relation of shell form to life habits of the Bivalvia (Mollusca). *Memoirs of the Geological Society of America*, **125**, 1–199.

SPAFFORD C. ACKERLY
Institut für Geologie und Paläontologie
Universität Tübingen
D7400 Tübingen, Germany

and

Department of Geology and Applied Geology
University of Glasgow
Glasgow G12 8QQ, UK

Present address:
Colorado Rocky Mountain School
Carbondale, CO 81623, USA

Typescript received 22 April 1991
Revised typescript received 4 February 1992

APPENDIX: LOCATING THE CENTRE AND PARAMETERS OF AN ELLIPSE

The following method was used to fit an ellipse to a set of points on the shell margin. The method is in two parts: (1) find the best-fit centre and radius of a circle, and (2) using the best-fit centre from step 1, find the best-fit major and minor axes of an ellipse.

1. Best-fit centre and radius of a circle

The non-linear regression technique is a method of successive approximation (see Snedecor and Cochran 1980), based on the equation for a circle:

$$(x_i - x_c)^2 + (y_i - y_c)^2 = r^2,$$

or,

$$(x_i - x_c)^2 + (y_i - y_c)^2 - r^2 = 0,$$

where the circle radius is r, the circle centre is at the location (x_c, y_c), and (x_i, y_i) are the coordinates of the ith point on the perimeter of the circle. An initial estimate of the position of the circle centre and the radius is provided, and the algorithm estimates a new centre and radius such that the left side of the equation tends towards zero. The new estimate is found by using x_c, y_c, and r, to produce a new matrix, u_i, v_i, w_i, from the equations:

$$\begin{aligned} u_i &= (x_i - x_c)^2 + (y_i - y_c)^2 - r^2, \\ v_i &= -2(x_i - x_c), \\ w_i &= -2(y_i - y_c), \end{aligned}$$

where v_i and w_i are the partial differentials of x_c and y_c respectively. A second-order linear regression is then applied to the values of u_i, v_i, and w_i, yielding an equation of the form:

$$u_i = b_0 + b_1 v_i + b_2 w_i,$$

where b_0, b_1, and b_2 are least-squares regression coefficients. The coefficients are used to provide new estimates of x_c, y_c, and r, according to:

$$\begin{aligned} r_{j+1} &= \text{sqr}\,(r_j^2 + b_0), \\ x_{c,j+1} &= x_{c,j} + b_1, \\ y_{c,j+1} &= y_{c,j} + b_2, \end{aligned}$$

where r_j is the original estimate and r_{j+1} is the new estimate, and similarly for x_c and y_c. The procedure is repeated until $r_{j+1} - r_j$ is less than a specified limit, and similarly for x_c and y_c (a limit of 10^{-8} was used in this analysis).

2. Best fit major and minor ellipse axes

The standard equation for an ellipse is:

$$x^2/a^2 + y^2/b^2 = r^2,$$

where $(2ar)$ is the length of the ellipse in the x direction, $(2br)$ is the length of the ellipse in the y direction, and a/b defines the aspect ratio of the ellipse. The ellipse equation is transformed to:

$$y_i^2 = b^2 r^2 - b^2 x_i^2 / a^2,$$

and a least-squares regression performed on the matrix of values (x_i, y_i), where (x_i, y_i) are points on the shell margin measured relative to the aperture centre (x_c, y_c), as found above. The regression coefficients b_0 and b_1 are used to find the ellipse parameters a and b, according to:

$$\begin{aligned} b_0 &= b^2 r^2, \\ b_1 &= -b^2/a^2, \end{aligned}$$

or

$$\begin{aligned} b &= \text{sqr}\,(b_0/r^2), \\ a &= \text{sqr}\,(-b^2/b_1), \end{aligned}$$

where r is the circle radius found above.